Ab Initio Quantum-Mechanical and Experimental Mechanistic Studies of Diels-Alder Reactions between Unsubstituted and Phenyl-Substituted Acetylenes and 1,2,4,5-Tetrazines

Jerzy Cioslowski,*,† J. Sauer,*,‡ J. Hetzenegger,‡ T. Karcher,‡ and T. Hierstetter‡

Contribution from the Department of Chemistry and Supercomputer Computations Research Institute, Florida State University, Tallahassee, Florida 32306-3006, and Universität Regensburg, Institut für Organische Chemie, 8400 Regensburg, Universitätstrasse 31, Postfach 397, Germany.
Received September 25, 1992

Abstract: 1,2,4,5-tetrazine (**2a**) undergoes thermal addition to phenylacetylene (**1b**) in dioxane with $\Delta H^{\ddagger}$ = 15.8 kcal/mol and $\Delta S^{\ddagger}$ = −31 cal/(mol·K). The activation parameters for the corresponding addition of **1b** to 3-phenyl-1,2,4,5-tetrazine (**2b**) are $\Delta H^{\ddagger}$ = 16.3 kcal/mol and $\Delta S^{\ddagger}$ = −31 cal/(mol·K). The (4+2)-cycloaddition of **2b** to **1b** yields a mixture (with the ratios of 90.5:9.5 in dioxane and 94.5:5.5 in acetonitrile) of 3,4-diphenylpyridazine (**6b**) and 3,5-diphenylpyridazine (**6c**). Detailed ab initio electronic structure calculations are carried out in order to explain these experimental findings, and the computed electronic wave functions are analyzed with the help of rigorous interpretive tools. At the MP2/6-311G** level, the activation energy for the Diels-Alder cycloaddition of acetylene (**1a**) to **2a** is estimated at 12.6 kcal/mol. The activation energy for the decomposition of the resulting intermediate (**4a**) to pyridazine (**6a**) and nitrogen (**7a**) is only 5.5 kcal/mol at the HF/6-31G* level. At the MP2/6-311G** level, the reaction barrier for the decomposition of **4a** is so small that the corresponding transition state cannot be located. The head-to-tail cycloaddition of **1b** to **2b**, which results in **6c** as a final product, is preferred to the head-to-head cycloaddition (leading to **6b**) by 0.9 kcal/mol at the HF/6-31G* level. However, when the attractive dispersion interactions between the phenyl rings are taken into account, formation of **6b** is found to be favored over that of **6c** by 4.0 kcal/mol, in agreement with the experimental observations. This unexpected conclusion provides the first documented example of regiospecificity being primarily controlled by the dispersion (attractive van der Waals) interactions.

Introduction

Diels-Alder reactions with inverse electron demand, first proposed by Bachmann and Deno,[1] involve electron-poor dienes and electron-rich dienophiles. These reactions, whose stereospecificity, regiospecificity, and solvent influence on the activation parameters closely parallel those of their "normal" counterparts, have found several applications in organic chemistry. In particular, symmetrical 1,2,4,5-tetrazine (**2a**) and its derivatives have proven to be versatile and very reactive components in (4+2)-cycloadditions to electron-rich dienophiles, such as acetylene (**1a**), phenylacetylene (**1b**), enol ethers, enamines, or ketene acetals, acting as the 2π-partners.[2]

Although a large number of high-quality ab initio electronic structure calculations have been carried out for species involved in both the normal and inverse Diels-Alder reactions,[3] only very recently it has become feasible to study with accurate quantum-mechanical methods bonding in systems composed of more than 20 atoms,[4] thus making it possible to interpret and understand experimental data on many cycloadditions of interest to organic chemists.

In this paper, we report on a combined experimental and theoretical study on two inverse-demand Diels-Alder reactions. The reaction I (Figure 1a) begins with a (4+2)-cycloaddition of 1,2,4,5-tetrazine (**2a**) to acetylene (**1a**), whereas the highly regiospecific reaction II (Figure 1b) involves 3-phenyl-1,2,4,5-tetrazine (**2b**) as the diene and phenylacetylene (**1b**) as the dienophile. In both cases, the addition is followed by elimination of the nitrogen molecule from the resulting intermediate, leading to the formation of (substituted) pyridazine.

Experimental Methods

Reaction of 2b with 1b To Form 6b and 6c. A solution of 1.02 g of 3-phenyl-1,2,4,5-tetrazine (**2b**) and 2.00 g of phenylacetylene (**1b**) in 15 mL of absolute dioxane was heated to 70 °C for 7 days. After another 0.60 g of **1b** was added and the reaction mixture was heated for 1 day, the solvent was removed in vacuo and the residue dried at 40 °C with an oil pump. The 250-MHz NMR showed a ratio of 93:7 for **6b**:**6c**. HPLC (reversed phase, 60% CH_3OH, 40% H_2O, internal standard 2-ethoxynaphthalene) gave a yield of 93% and a ratio of 90.5:9.5 for **6b**:**6c**.

When the above reaction is performed in acetonitrile, the corresponding product ratio is 94.5:5.5 (by HPLC).

Separation of pure 3,4-diphenylpyridazine (**6b**) from 3,5-diphenylpyridazine (**6c**) is possible by flash chromatography (h = 35 cm, d = 3.5 cm, silica gel, ethyl acetate/n-hexane = 1:1) with a TLC control (**6b**: R_f = 0.29. **6c**: R_f = 0.57). Final crystallization from cyclohexane gave pure **6b** (83%, mp 104-105 °C[5] and **6c** (3.7%, mp 140-142 °C[6]).

In a similar reaction, 1,2,4,5-tetrazine (**2a**) and **1b** afforded pure 4-phenylpyridazine with an 85% yield.

Kinetic Measurements. Tetrazines **2a** and **2b** were sublimed under reduced pressure several times. Phenylacetylene (**1b**; FLUKA) still contained 2-3% of styrene, which because of its higher reactivity had to be removed. To accomplish this, **1b** (4.60 g dissolved in 20 mL of CH_2Cl_2) was treated with Br_2 (1.90 g in 10 mL of CH_2Cl_2) for 4 h. The organic layer was washed three times with 3% NaOH, dried over Na_2SO_4, and distilled, yielding 3.10 g of pure **1b** (<0.1% of styrene by GC).

Solutions of tetrazines and phenylacetylene in dioxane or acetonitrile that were prepared for the kinetic runs contained (1.5-2.2) × 10^{-2} mol/dm^3 tetrazine and a 10- to 25-fold excess of phenylacetylene. The solutions were divided into 1-2 mL samples, sealed in little glass vessels, and heated to the reaction temperature. The samples (usually 20) were taken at appropriate intervals, and the reaction progresses were followed by monitoring the $n \rightarrow \pi^*$ transition of the tetrazines around 540 nm to cover 5-90% of the reaction. Parallel runs reproduced the reaction rate values within ±2%.

Theoretical Methods. All calculations were performed on the CRAY Y-MP4/32 supercomputer located at FSU/SCRI with the GAUSSIAN 90[7] suite of programs. The 6-31G** and 6-311G** basis sets were used in conjunction with full geometry optimizations at the HF and MP2 levels. The total energies of the systems under study (Figure 1) are listed

† Florida State University.
‡ Universität Regensburg.

(1) Bachmann, W. E.; Deno, N. C. *J. Am. Chem. Soc.* **1949**, *71*, 3062.
(2) For a recent review see: Sauer, J.; *Bull. Soc. Chim. Belg.* **1992**, *101*, 521.
(3) For a recent extensive review see: Houk, K. N.; Li, Y.; Evanseck, J. D. *Angew. Chem., Int. Ed. Engl.* **1992**, *31*, 682.
(4) For a recent review see: Cioslowski, J. Ab Initio Calculations on Large Molecules: Methodology and Applications. In *Reviews in Computational Chemistry*; Lipkowitz, K. B., Boyd, D. B., Eds.; VCH Publishers: New York, 1993; Vol. 4.
(5) Almström, G. K. *Liebigs Ann. Chem.* **1913**, *400*, 131.
(6) Breslow, R.; Eicher, T.; Krebs, A.; Peterson, R. A.; Posner, J. *J. Am. Chem. Soc.* **1965**, *87*, 1320.
(7) Frisch, M. J.; Head-Gordon, M.; Trucks, G. W.; Foresman, J. B.; Schlegel, H. B.; Raghavachari, K.; Robb, M.; Binkley, J. S.; Gonzalez, C.; Defrees, D. J.; Fox, D. J.; Whiteside, R. A.; Seeger, R.; Melius, C. F.; Baker, J.; Martin, R. L.; Kahn, L. R.; Stewart, J. J. P.; Topiol, S.; Pople, J. A. *GAUSSIAN 90*, Revision F; GAUSSIAN, Inc.: Pittsburgh, PA, 1990.

0002-7863/93/1515-1353$04.00/0

Table I. Total Energies of the Molecules Under Study

molecule	structure[a]	total energy[b] (au) HF/6-31G**	MP2/6-311G**
C_2H_2	**1a**	-76.821 837	-77.148 394
$C_2H_2N_4$	**2a**	-294.596 375	-295.712 573
TS1	**3a**	-371.351 148	-372.842 663
$C_4H_4N_4$	**4a**	-371.457 107	-372.929 690
TS2	**5a**	-371.445 834	[d]
$C_4H_4N_2$	**6a**	-262.657 067	-263.703 089
N_2	**7**	-108.943 949	-109.334 062
$C_6H_5{\cdot}CCH$	**1b**	-306.389 247	[d]
$C_6H_5{\cdot}C_2HN_4$	**2b**	-524.162 273	[d]
o-TS1	**3b**	-830.475 440	[d]
o-$(C_6H_5)_2{\cdot}C_4H_2N_4$	**4b**	-830.568 872	[d]
o-$(C_6H_5)_2{\cdot}C_4H_2N_2$	**6b**	-721.769 934	[d]
m-TS1	**3c**	-830.476 957	[d]
m-$(C_6H_5)_2{\cdot}C_4H_2N_4$	**4c**	-830.574 004	[d]
m-$(C_6H_5)_2{\cdot}C_4H_2N_2$	**6c**	-721.777 171	[d]
"*o*-$(C_6H_6)_2$ sep"	**8b**	-461.427 279[c]	-463.008 943[c]
"*o*-$(C_6H_6)_2$"	**9b**	-461.421 497[c]	-463.011 281[c]
"*m*-$(C_6H_6)_2$ sep"	**8c**	-461.427 474[c]	-463.009 078[c]
"*m*-$(C_6H_6)_2$"	**9c**	-461.427 453[c]	-463.009 461[c]

[a] See Figure 1. [b] Energies corresponding to fully optimized geometries at the indicated level unless stated otherwise. [c] HF/6-31G** and MP2/6-31G** energies; see text for explanation of the geometries chosen. [d] Not available.

Table II. Relative Energies of the Molecules Pertinent to Reaction I

structure[a]	relative energy (kcal/mol) HF/6-31G**	HF/6-31G** + ZPE[b]	MP2/6-311G**	"best"[c]
reactants **1a** + **2a**	0.0	0.0	0.0	0.0
TS1 **3a**	42.1	43.2	11.5	12.6
intermediate **4a**	-24.4	-20.1	-43.1	-38.8
TS2 **5a**	-17.3	-14.6	[d]	[d]
products **6a** + **7**	-114.7	-113.2	-110.6	-109.1

[a] See Figure 1 for the numbering of structures. [b] At 298 K, uncorrected vibrational energies used. [c] MP2/6-311G** energy with the ZPE energy calculated at the HF/6-31G** level. [d] Not available.

in Table I. The energy-derivative ("relaxed") density matrices[8] were utilized in calculations of the MP2 properties. The computed electronic wave functions were analyzed with rigorous interpretive tools.[9] In particular, the electron densities were analyzed within the framework of the topological theory of atoms in molecules.[10] In all of the systems under study, no evidence was found of either "weak" bond paths[11] or interaction lines characteristic of steric repulsions.[12] For this reason, all of the molecules studied can be regarded as being free from steric crowding. The Bader atomic charges[10] and atomic overlap matrices (AOMs)[13] were evaluated by numerical integrations performed with a vectorized version[14] of the PROAIM program.[13] In addition, the GAPT atomic charges[15] were computed at the HF/6-31G** level. The covalent bond orders[16] were calculated from the AOM-localized natural orbitals.[17] Finally, the individual reaction steps were characterized by reaction parameters[18] obtained with the NOEL program.[19]

Table III. Molecular Similarities and Reaction Parameters for Reaction I[a]

reaction step[b]	NOEL[c] (A,B)	(A,TS)	(B,TS)	reaction parameters[d] α	β	γ
1a + **2a** → **4a**	43.677	49.324	45.231	1.671	-0.199	-0.225
4a → **6a** + **7**	44.498	51.588	46.817	1.513	-0.274	-0.865

[a] All data calculated at the HF/6-31G** level. [b] See Figure 1 for the numbering of structures. [c] A are the reactants, TS are the transition states, and B are the products; (A,A) = (B,B) = (TS,TS) = 56.000. [d] α is the isosynchronicity, β is the proximity of the transition state to the reactants, and γ is the exothermicity.

Table IV. AOM-Derived Covalent Bond Orders in the Molecules Pertinent to the First Step of Reaction I[a]

bond[b]	structure[b] **1a** + **2a**	**3a**	**4a**
C_1–C_2, C_3–C_4	0.000	0.153	0.982 (0.978)
C_2–C_3	2.741	2.426	1.723 (1.851)
C_1–N, C_1–N_3, C_4–N_2, C_4–N_4	1.172	1.140	0.873 (0.899)
N_1–N_2, N_3–N_4	1.543	1.601	2.000 (2.103)
C_1–H_1, C_4–H_4	0.903	0.905	0.923 (0.950)
C_2–H_2, C_3–H_3	0.980	0.940	0.958 (1.002)

[a] Bond orders calculated at the MP2/6-311G** level (the HF/6-31G** values in parentheses) with the values averaged between two Kekule structures for **2a** and **3a**. [b] See Figure 2 for the atom numbering in individual structures.

Table V. Atomic Charges in the Molecules Pertinent to the First Step of Reaction I[a]

atom[b]	structure[b] **1a** + **2a**	**3a**	**4a**
C_1, C_4	0.982	0.788	0.327 (0.626) [0.180]
C_2, C_3	-0.152	-0.121	-0.024 (0.042) [0.033]
N_1, N_2, N_3, N_4	-0.537	-0.458	-0.220 (-0.340) [-0.120]
H_1, H_4	0.093	0.080	0.069 (0.001) [0.013]
H_2, H_3	0.152	0.170	0.068 (0.011) [0.079]

[a] Bader atomic charges calculated at the MP2/6-311G** level (the HF/6-31G** values in parentheses), followed by the HF/6-31G** GAPT atomic charges in square brackets. [b] See Figure 2 for the atom numbering in individual structures.

Results and Discussion

Addition of Acetylene to 1,2,4,5-Tetrazine. The Diels–Alder 1,4-cycloaddition of acetylene (**1a**) to 1,2,4,5-tetrazine (**2a**) comprises the first step of reaction I. The HF/6-31G** calculations locate the respective transition state TS1 (**3a**) at 42.1 kcal/mol above the reactants (Table II). However, inclusion of electron correlation drastically lowers the reaction barrier, resulting in the value of $\Delta E^{\ddagger}$ equal to only 11.5 kcal/mol at the MP2/6-311G** level. This figure is increased only slightly by the zero-point energies (ZPEs).

In the transition state, the acetylene and 1,2,4,5-tetrazine moieties are markedly distorted from their equilibrium geometries (Figure 2). The hydrogen atoms of acetylene are bent outward from the approaching 1,2,4,5-tetrazine molecule, which in turn buckles its ring in a way that reduces the distances between its 1,4-carbon atoms and the carbon atoms of acetylene. The overall visual assessment of the structure displayed in Figure 2 is that TS1 is slightly early. This qualitative impression is confirmed by the computed values of the reaction parameters α, β, and γ[18] (Table III) calculated with the help of a quantitative similarity measure known as NOEL.[19] Since the formation of 2,3,5,6-tetraazabarrelene (**4a**) is an exothermic reaction, the exothermicity parameter γ is negative. The parameter β that measures the proximity of the transition state to the reactants is slightly negative, indicating a rather early transition state. This is also reflected in the similarity indices that suggest that TS1 resembles the reactants more than the product, (A, TS) > (B, TS). The calculated isosynchronicity parameter α is quite small, which means that most of the structural changes that accompany the cycloaddition under study occur in the proximity to the reaction center.

(8) Salter, E. A.; Trucks, G. W.; Fitzgerald, G.; Bartlett, R. J. *Chem. Phys. Lett.* **1987**, *141*, 61. Trucks, G. W.; Salter, E. A.; Sosa, A.; Bartlett, R. J. *Chem. Phys. Lett.* **1988**, *147*, 359.
(9) Cioslowski, J.; Surjan, P. R. *J. Mol. Struct.* **1992**, *255*, 9.
(10) Bader, R. F. W. *Atoms in Molecules: A Quantum Theory*; Clarendon Press: Oxford, 1990.
(11) Cioslowski, J.; Mixon, S. T.; Edwards, W. D. *J. Am. Chem. Soc.* **1991**, *113*, 1083.
(12) Cioslowski, J.; Mixon, S. T. *J. Am. Chem. Soc.* **1992**, *114*, 4382.
(13) Biegler-König, F. W.; Bader, R. F. W.; Tang, T. H. *J. Comput. Chem.* **1982**, *3*, 317.
(14) Cioslowski, J. VECAIM: A Vectorized PROAIM. Supercomputer Computations Research Institute, Florida State University, 1992.
(15) Cioslowski, J. *J. Am. Chem. Soc.* **1989**, *111*, 8333. Cioslowski, J.; Hamilton, T.; Scuseria, G.; Hess, B. A., Jr.; Hu, J.; Schaad, L. J.; Dupuis, M. *J. Am. Chem. Soc.* **1990**, *112*, 4183.
(16) Cioslowski, J.; Mixon, S. T. *J. Am. Chem. Soc.* **1991**, *113*, 4142.
(17) Cioslowski, J. *Int. J. Quantum Chem.* **1990**, *S24*, 15.
(18) Cioslowski, J. *J. Am. Chem. Soc.* **1991**, *113*, 6756.
(19) Cioslowski, J.; Fleischmann, E. D. *J. Am. Chem. Soc.* **1991**, *113*, 64.

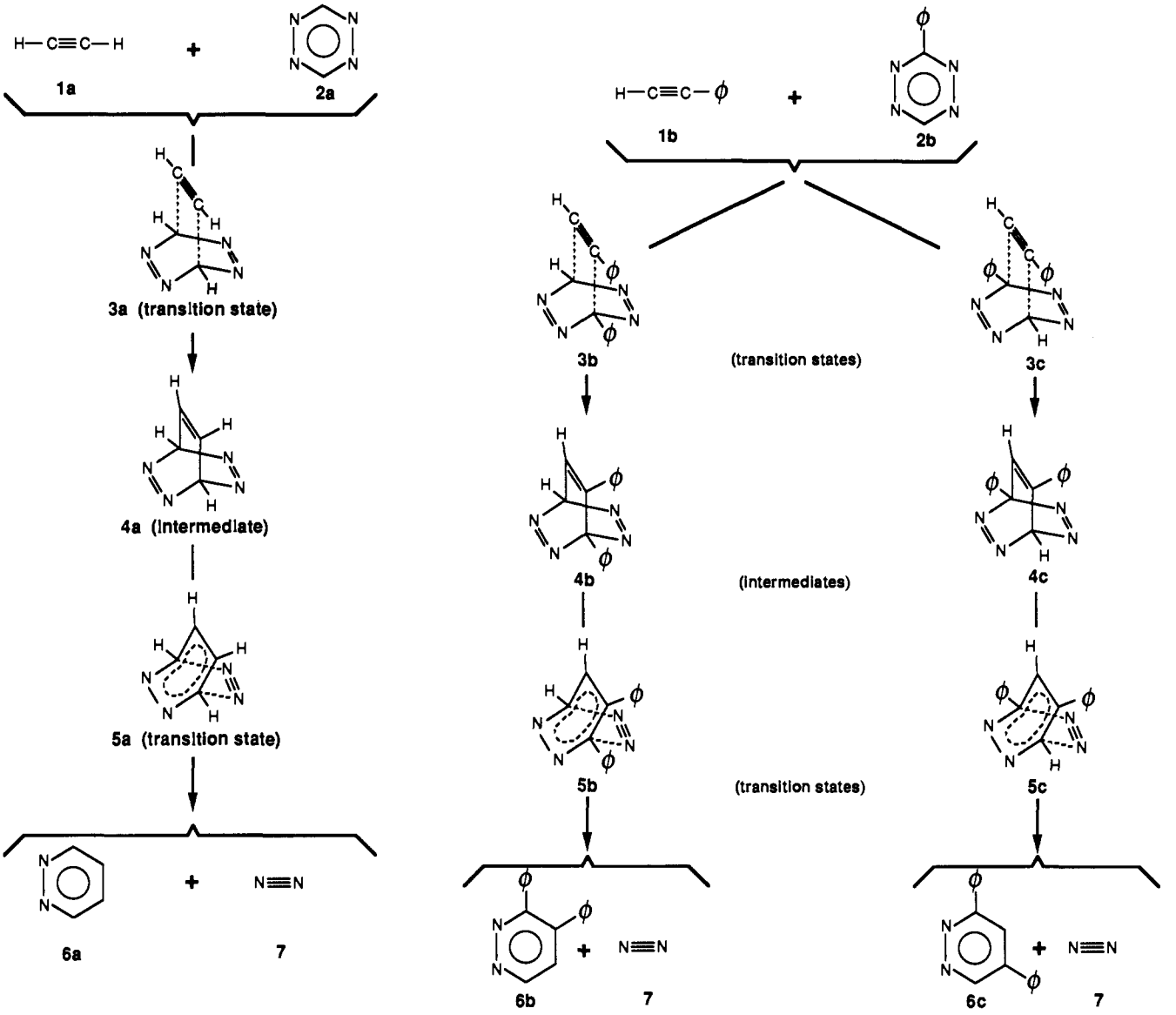

Figure 1. Chemical systems under study: (a, left) reaction I; (b, right) reaction II.

The values of the MP2/6-311G** covalent bond orders, listed in Table IV, are in agreement with the above observations. The bond order of the triple bond in acetylene, which is equal to 2.741, decreases somewhat in TS1 but still retains quite a large value of 2.426. Both the weakening of the carbon–nitrogen bonds of 1,2,4,5-tetrazine and the strengthening of its nitrogen–nitrogen bonds are even less pronounced. The new carbon–carbon bonds only begin to form in TS1, as reflected by the low values of 0.153 for the respective bond orders. These bond orders increase to 0.982 in the product (**4a**), indicating the presence of single bonds. The other bond orders in **4a** are in accordance with the structure in which the NN fragments possess double bonds and are linked to the rest of the molecule through polarized single bonds. One should note that the bond orders calculated at the HF/6-31G** level, listed in Table IV for comparison, are overestimated by only a small amount.

The atomic charges in the species relevant to the first step of reaction I are displayed in Table V. As expected, the bond polarity is C^-–H^+ in the acetylene molecule and decreases upon the formation of **4a**. The same is true about the polarities of the C–N bonds in 1,2,4,5-tetrazine. Inclusion of electron correlation appears to decrease the Bader atomic charges substantially. The relative magnitudes of the GAPT atomic charges follow those of the Bader ones.

Decomposition of 2,3,5,6-Tetraazabarrelene to Pyridazine and Nitrogen. The second step of reaction I involves elimination of the nitrogen molecule (7) from the intermediate (**4a**), leading to the formation of pyridazine (**6a**). The activation energy corresponding to the transition state TS2 (**5a**) is estimated at only 5.5 kcal/mol at the HF/6-31G** level (Table II). The reaction is very exothermic, as reflected by the calculated energy differences between the products and the reactant (HF/6-31G**: 93.1 kcal/mol. MP2/6-311G**: 67.5 kcal/mol. "best": 70.3 kcal/mol. See Table II) and by the strongly negative value of the exothermicity parameter γ (Table III). The HF/6-31G** transition state appears to be early, as indicated by the negative value of β.

Despite several attempts, we were unable to locate the transition state TS2 at the MP2/6-311G** level. We believe that this is due to its extreme proximity to the reactant. It is very probable that at the higher levels of theory both the intermediate **4a** and the transition state **5a** might not even be the stationary points on the potential energy hypersurface. It is therefore conceivable that reaction I actually involves the addition of acetylene and the elimination of nitrogen occurring in a one-step, yet asynchronous, process.

Diels–Alder Reaction between Phenylacetylene and Phenyl-1,2,4,5-tetrazine. Our kinetic studies of the reaction between **1b** and **2a** in dioxane show a low activation enthalpy of 15.8 kcal/mol (Table VI), in agreement with the theoretical predictions for the prototype reaction I. Replacing **2a** by 3-phenyl-1,2,4,5-tetrazine (**2b**) increases the experimental activation enthalpy by only 0.5

Table VI. Kinetic Data for the (4+2)-Cycloadditions of Phenylacetylene to 1,2,4,5-Tetrazine and 3-Phenyl-1,2,4,5-tetrazine

reactions[a]	solvent	$10^4 k_2$[b] (dm^3/(mol·s))	$\Delta H^{\ddagger}$[c] (kcal/mol)	$\Delta S^{\ddagger}$[c] (cal/(mol·K))
1b + **2a**	dioxane	4.84	15.8 ± 0.2	−31 ± 1
1b + **2b**	dioxane	1.70	16.3 ± 0.2	−31 ± 1
	acetonitrile	3.19	[d]	[d]

[a] See Figure 1 for the numbering of structures. [b] At 90 °C. [c] Measured between 80 and 100 °C. [d] Not available.

Table VII. Relative Energies of the Molecules Pertinent to Reaction II

structure[a]	relative energy (kcal/mol) HF/6-31G**	"corrected I"[b]	"corrected II"[c]
reactants **1b** + **2b**	0.0	0.0	0.0
TS1 **3b**	47.7	18.2	13.1
intermediate **4b**	−10.9	−25.3	[d]
products **6b** + **7**	−101.9	−96.3	[d]
TS1 **3c**	46.8	17.3	17.1
intermediate **4c**	−14.1	−28.5	[d]
products **6c** + **7**	−106.4	−100.8	[d]

[a] See Figure 3 for the HF/6-31G** optimized geometries of the individual structures, note that the data for TS2 are not available. [b] Corrected by E("best") − E(HF/6-31G**) for the respective unsubstituted structure. [c] See text for explanation. [d] Not available.

kcal/mol. Even more importantly, as already mentioned in the experimental section of this paper, 3,4-diphenylpyridazine (**6b**) is produced almost exclusively in this reaction, which we call here reaction II.

Reaction II involves either a head-to-head or head-to-tail Diels–Alder cycloaddition of **1b** to **2b** as its first step, leading to the 2,3,5,6-barrelene intermediates **4b** and **4c**, respectively (Figures 1 and 3). At the HF/6-31G** level, the corresponding transition states **5b** and **5c** (Figure 1) for the elimination of the nitrogen molecule, which constitutes the second step of reaction II, cannot be located, most probably due to their proximities to the intermediates **4b** and **4c** and the resulting very low reaction barrier. On the other hand, geometries of the transition states **3b** and **3c** can be optimized (Figure 3). However, at the HF/6-31G** level, the transition state for the head-to-head cycloaddition (**3b**) is calculated (Table VII) to lie 0.9 kcal/mol above that for the head-to-tail cycloaddition (**3c**), incorrectly predicting the preferential formation of 3,5-diphenylpyridazine (**6c**).

The discrepancy between this theoretical prediction and the experimental facts could in principle originate from either the entropic effects or the neglect of electron correlation. The former possibility has to be rejected, as the entropic terms are estimated (based on the moments of inertia corresponding to the calculated HF/6-31G** geometries) to contribute less than 0.4 kcal/mol to the difference in the activation enthalpies in question. Concerning the latter possibility, direct MP2 calculations on the transition states **3b** and **3c** are not currently feasible because of the size of these systems. However, by assuming their additivity, reasonably accurate, indirect estimates of the electron correlation contributions to the activation energies can be obtained. First of all, the differences between the "best" and the HF/6-31G** energies of the transition state **3a** can be used to correct the activation energies for the neglect of correlation energy contributions pertinent to the tetraazabarrelene moiety. This correction lowers the activation energies corresponding to **3b** and **3c** by the same amount and therefore does not alter the conclusions concerning regiospecificity (see the relative energies listed under "corrected I" in Table VII).

The other, more important correction comes from the neglected electron correlation effects that originate from the interactions between the phenyl fragments of the phenylacetylene and phenyl-1,2,4,5-tetrazine moieties. In particular, it should be pointed out that the Hartree–Fock energies of **3b** and **3c** contain the purely electronic contributions (those usually attributed to "orbital interactions") as well as the steric repulsions between the phenyl fragments. Missing, however, at the Hartree–Fock level are the contributions due to the dispersion forces between the phenyl fragments. These contributions can be quite accurately (probably within ±0.2 kcal/mol) estimated by considering the total energies of supermolecules, denoted by "*o*-$(C_6H_6)_2$" (**9b**) and "*m*-$(C_6H_6)_2$" (**9c**) in Table I. The supermolecules (**9b**) and (**9c**) consist of two benzene molecules with the geometries and mutual positions identical with those of the phenyl fragments in the transition states **3b** and **3c**, respectively. Differences between the Hartree–Fock energies of the supermolecules and the energies of the corresponding isolated benzene molecules, denoted by "*o*-$(C_6H_6)_2$ sep" (**8b**) and "*m*-$(C_6H_6)_2$ sep" (**8c**) in Table I, yield the steric repulsion contributions to the activation energies. The sums of the energy contributions due to steric repulsion and the attractive dispersion interactions are given by the analogous differences in the MP2 energies, making it possible to estimate the magnitudes of the latter contributions. These contributions, when added to the "corrected I" energies in Table VII, yield the final "corrected II" activation energies. Finally, the energy contributions arising from purely electronic effects are obtained by subtracting the sums of the steric repulsion and the attractive dispersion contributions from the differences between the respective corrected activation energies of the reactions I and II.

Table VIII. Estimated Contributions to the Differences in Activation Energies for Reactions I and II

direction	contribution to $\Delta(\Delta E^{\ddagger})$[a] (kcal/mol) electronic	steric repulsion	dispersion energy	total
head-to-head	2.0	3.6	−5.1	0.5
head-to-tail	4.7	0.0	−0.2	4.5

[a] See text for explanation.

As one concludes from inspection of the results presented in Table VIII, for the head-to-head cycloaddition, the purely electronic effects account for 2.0 kcal/mol in the difference between the activation energies of the first steps of reactions I and II. The steric repulsions between the phenyl fragments increase the reaction barrier by an additional 3.6 kcal/mol. However, most of these gains are wiped out by the dispersion interactions between the phenyl fragments, resulting in the reaction barrier that is higher than that of reaction I by only 0.5 kcal/mol. It is therefore fair to say that the van der Waals attractive interactions play a decisive role in determining the activation energy for the head-to-head Diels–Alder cycloaddition of phenylacetylene (**1b**) to phenyl-1,2,4,5-tetrazine (**2b**) by providing a stabilizing effect that is sufficiently large to almost totally overcome the sum of contributions due to steric repulsions and electronic effects. The net interaction energy between the phenyl fragments is calculated to be equal to −1.5 kcal/mol. This is a reasonable estimate, taking into account that the experimental dimerization energy of benzene is about −2.0 kcal/mol,[20] although the minimal energy orientation of the benzene rings corresponds to a T-shaped dimer. It should be also recalled that the importance of the dispersion interactions to structures of organic compounds is well documented in chemical literature, the calculations on ferrocene by Park and Almlöf[21] being one of the recent examples. In these calculations, the attractive interactions between the cyclopentadienyl rings were found to shorten the iron–ligand distances by as much as 0.03 Å.

Returning to the discussion on the Diels–Alder cycloaddition, we have to point out that, in contrast with the aforementioned case, for the head-to-tail cycloaddition, the bulk of increase in the activation energy comes from the electronic effects. This is understandable considering the large distance between the phenyl fragments in **3c** (see Figure 3).

Finally, we would like to mention that the semiempirical MNDO-PM3 calculations are incapable of correctly predicting either the activation energy or regiospecificity of reaction II. The calculated enthalpy of activation (Table IX) is grossly overesti-

(20) Krause, H.; Ernstberger, B.; Neusser, H. J. *Chem. Phys. Lett.* **1991**, *184*, 411.
(21) Park, C.; Almlöf, J. *J. Chem. Phys.* **1991**, *95*, 1829.
(22) Stewart, J. J. P. *J. Comput. Chem.* **1989**, *10*, 209, 221.

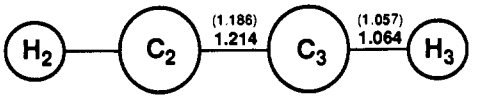

1a

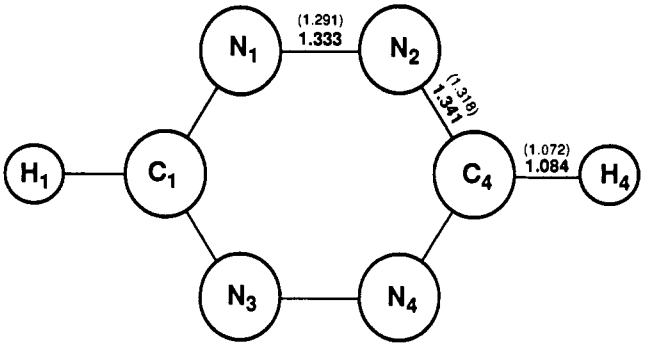

2a

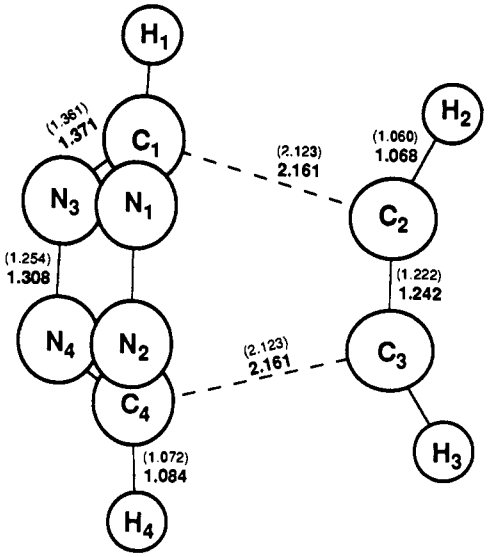

3a

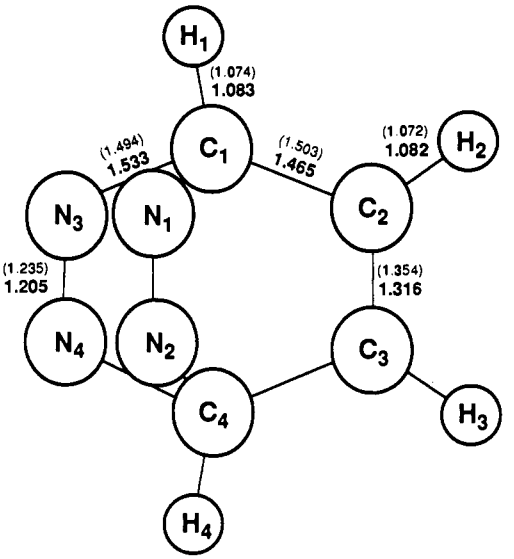

4a

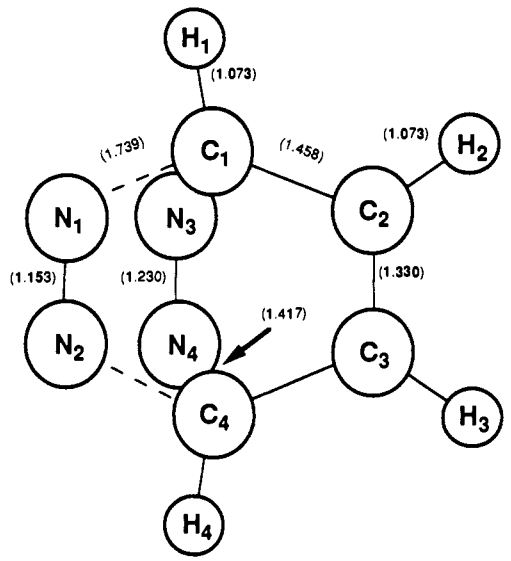

5a

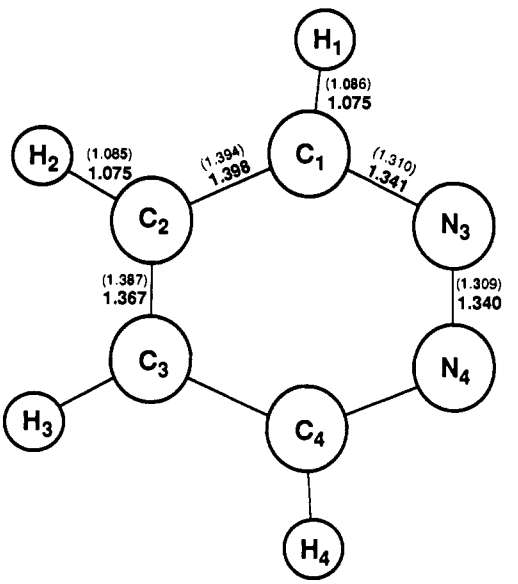

6a

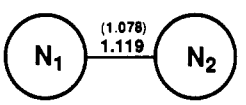

7

Figure 2. Selected MP2/6-311G** optimized bond lengths (in Å) in the molecules pertinent to reaction I. The HF/6-31G** values are given in parentheses.

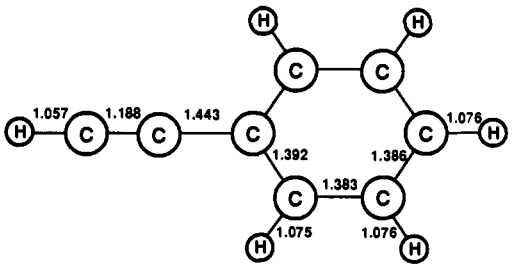

1b

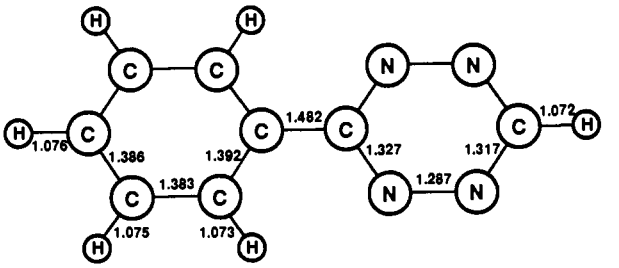

2b

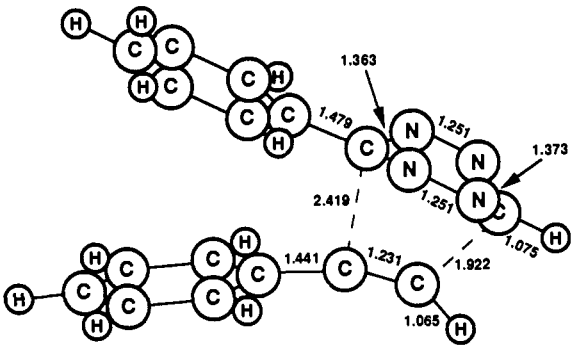

3b

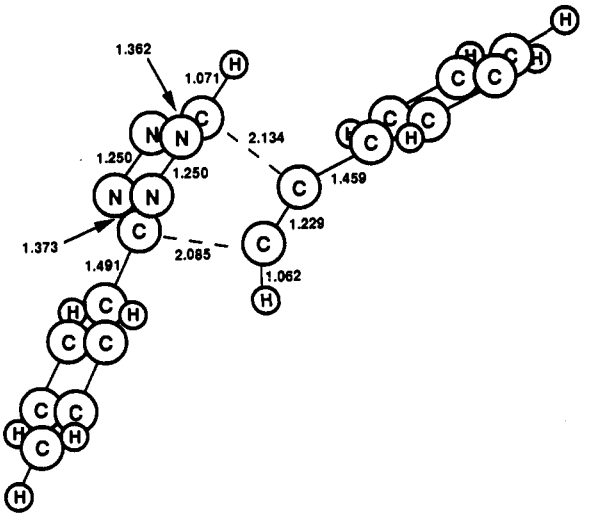

3c

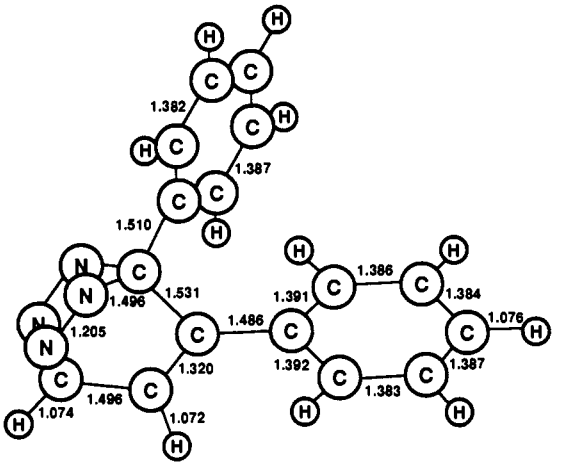

4b

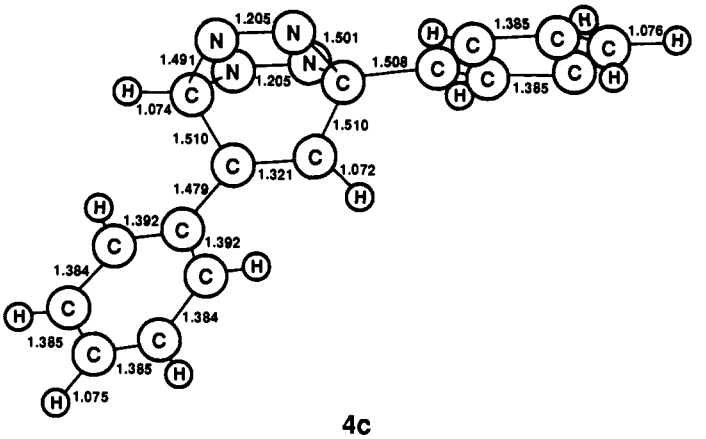

4c

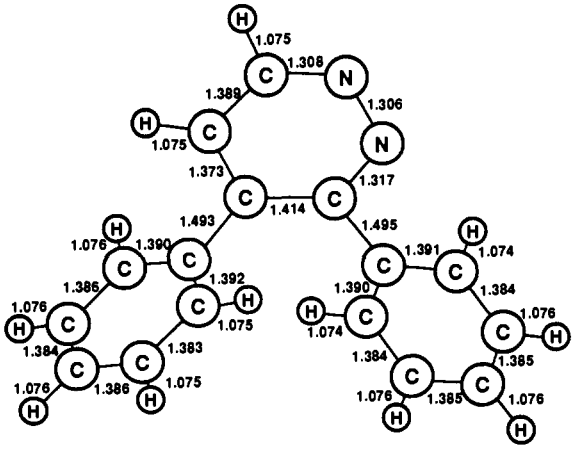

6b

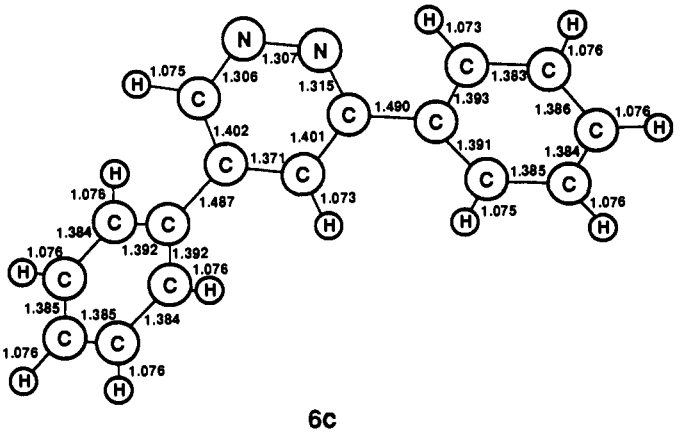

6c

Figure 3. Selected HF/6-31G** optimized bond lengths (in Å) in the molecules pertinent to reaction II.

Table IX. MNDO-PM3 Heats of Formation of the Molecules Pertinent to Reaction II

structure[a]	ΔH_f^b (kcal/mol)
1b	119.0
2b	74.7
3b	234.1 (40.4)
3c	231.6 (37.9)
4b	173.9 (-19.8)
4c	173.4 (-20.3)

[a] See Figure 1. [b] Enthalpies relative to **1b** + **2b** are listed in parentheses.

mated, and the formation of **6c** is favored over that of **6b** by 2.5 kcal/mol. We believe that this failure of the MNDO-PM3 method can be directly attributed to the absence of dispersive interactions and the resulting exaggeration of the repulsion between the phenyl rings of the reactants.

Conclusions

The experimental and theoretical data presented above allows us to conclude that Diels-Alder cycloaddition is the rate-determining step for both reactions I and II. The addition involves a quite early transition state with the activation energy estimated at about 13 kcal/mol by the theoretical methods, in good agreement with the measured activation enthalpy of ca. 16 kcal/mol. In contrast, our calculations indicate that the second steps of both reactions I and II have either a very low reaction barrier or no barrier whatsoever.

For the reaction II, the formation of 3,4-diphenylpyridazine is preferred over that of 3,5-diphenylpyridazine by the estimated difference in the activation energies of 4.0 kcal/mol. The regiospecificity of reaction II cannot be predicted correctly at the HF level. However, the MP2 calculations provide the right answer, as they include the attractive dispersion interactions between the phenyl rings of the reactants, which are neglected at the Hartree-Fock level of theory. Surprisingly, the regiospecificity of reaction II is controlled primarily by the dispersion interactions, where out of the 4.0 kcal/mol difference in $\Delta E^{\ddagger}$, an estimated 2.7 kcal/mol comes from the purely electronic effects, -3.6 kcal/mol from steric repulsions, and 4.9 kcal/mol from the dispersive attraction between the phenyl rings.

The semiempirical MNDO-PM3 method is incapable of predicting either the activation energy or the regiospecificity of reaction II correctly. We believe that, by documenting the importance of including the attractive dispersion interactions in calculations aimed at prediction of rates and specificities of cycloadditions, an issue which has been mostly neglected in the chemical literature, the aforedescribed research will contribute to better understanding of the factors that influence these reactions.

Acknowledgment. This work was partially supported by the Deutsche Forschungsgemeinschaft (DFG), Fonds der Chemischen Industrie, the National Science Foundation under Contract CHE-9015566, the Camille and Henry Dreyfus Foundation New Faculty Award Program, and the Florida State University through time granted on its Cray Y-MP digital computer. The authors thank Dr. S. T. Mixon for the critical comments on the manuscript.

Cyclopentenone Formation via Hydrogen Activation in the Reactions of Chromium Carbene Complexes with Alkynes[1]

Cynthia A. Challener,[†,2a] William D. Wulff,[*,†] Benjamin A. Anderson,[†] Steve Chamberlin,[†,2b] Katherine L. Faron,[†,2a] Oak K. Kim,[†] Christopher K. Murray,[†] Yao-Chang Xu,[†] Dominic C. Yang,[†,2a] and Stephen D. Darling[‡]

Contribution from the Department of Chemistry, Searle Chemistry Laboratory, The University of Chicago, Chicago, Illinois 60637, and Department of Chemistry, University of Akron, Akron, Ohio 44325. *Received July 2, 1992*

Abstract: The reactions of alkyl chromium carbene complexes with alkynes have been found to give cyclopentenones. Mechanisms are proposed to account for the formation of these products that involve metal hydride intermediates. As has been previously reported for tungsten, molybdenum alkyl complexes have been found to give 1,3-dienes rather than cyclopentenones. The difference between chromium and molybdenum and tungsten may be that a metal hydride intermediate can re-add to an olefin in the case of chromium rather than undergo reductive elimination. A mechanism for the formation of cyclopentenones involving a free vinylketene was ruled out on the basis of an experiment in which the free vinylketene was generated via thermolysis of a cyclobutenone and found not to give a cyclopentenone product but rather an intramolecular [2 + 2] cycloadduct.

The coupling reactions of alkyl-substituted transition metal carbene complexes and alkynes have been known for some time.[3] The first reaction of this type involving activation of an α-hydrogen of the alkyl substituent was reported by Macomber in 1984.[4] He reported that (methylmethoxycarbene)pentacarbonyltungsten (**1a**, R = H) reacts with alkynes to provide moderate yields of 1,3-dienes (**2**) or the corresponding enones (**3**) after hydrolysis. Unlike the case for tungsten, there are no known reactions of alkyl-substituted molybdenum or chromium complexes with alkynes that involve activation of an α-hydrogen.[5] We report herein that all of the group 6 metals will react with acetylenes to give products resulting from activation of an α-hydrogen and that chromium

Scheme I

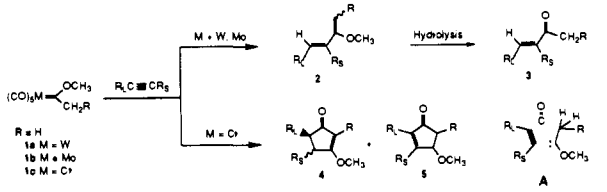

complexes uniquely produce the cyclic cyclopentenones **4** and **5** from this process.[1,6]

[†] The University of Chicago.
[‡] University of Akron.

(1) A preliminary account of this work was presented at the American Chemical Society National Meeting in Dallas, Texas, on April 9-14, 1989, ORG 185.

0002-7863/93/1515-1359$04.00/0